Journal of Applied Mechanics and Technical Physics, Vol. 44, No. 4, pp. 522–531, 2003

SOME FEATURES OF A TURBULENT SEPARATED FLOW AND HEAT TRANSFER BEHIND A STEP AND A RIB. 2. HEAT TRANSFER IN A SEPARATED FLOW

V. I. Terekhov, N. I. Yarygina, and R. F. Zhdanov

UDC 536.24

Results of an experimental study of heat transfer in a separated flow behind a step and a rib are presented. The influence of the obstacle height (H = 6–30 mm) on heat and mass transfer and the structure of the thermal boundary layer is studied. The features of heat transfer in recirculation and relaxation zones of the separated flow are analyzed, and the effect of separation on intensification and suppression of turbulent heat transfer is determined.

Key words: *experimental study, separated flows, turbulent flow, heat transfer, temperature distribution, step, rib, secondary vortex region.*

Introduction. Investigation of separated flows behind a step and behind a transverse obstacle is associated with certain difficulties [1]. Under these conditions, it is necessary to use an experiment to extend the database on turbulent separated flows, which allows one to improve numerical models. Only precise information on the flow structure and heat transfer will allow one to evaluate how accurately the numerical prediction reflects real thermal phenomena in separated flows.

Many papers deals with experimental investigations of heat transfer in the case of flow separation behind various obstacles. One should note reviews [2–5] and detailed studies [6–10], which form the basis for verification of most theoretical models. Attempts of empirical generalization of experimental data on the maximum heat transfer with various approaches used to choose the governing parameters were made [11, 12].

The mechanism of the heat- and mass-transfer processes during flow separation, however, has not been adequately studied. The separated flow is affected by a large number of factors, the main of them being the obstacle shape, degree of channel expansion, flow history, and external turbulence. The results of the present work supplement the database of experimental results obtained by various authors.

An analysis of the basic papers reveals a contradiction in available experimental data on heat transfer in separated flows. The measured results on heat transfer and dynamic characteristics of the separated flow behind a step are described in [8]. Results of numerous numerical models were compared with the experimental data of this work. Still, its drawbacks are inadequate investigation of the secondary zone, nonmeasured step height, and absence of a comparative analysis with data for reattaching flows behind obstacles of different geometry.

It should be noted that there is no unified opinion on the location (with respect to the flow-reattachment region) of the maximum heat-transfer coefficient behind both the step and the rib. In the experiments of [8, 13–15], the heat-transfer maximum is located closer to the step with respect to the reattachment region. There are experiments where the maximum heat-transfer coefficient is observed in the reattachment region [7, 16] or downstream from it [10, 17]. On a flat plate with a blunted leading edge, the heat-transfer coefficient reaches the maximum in the reattachment region [18]. Dyban et al. [19] note that the coordinates of the heat-transfer maximum can differ from the coordinates of the reattachment point, depending on the obstacle shape. It is argued that the maximum heat-transfer coefficient is located upstream of the reattachment region approximately by two calibers in the case of separation on a horizontal plate with an obstacle, by one caliber in the case of a plate with sharp

Kutateladze Institute of Thermophysics, Siberian Division, Russian Academy of Sciences, Novosibirsk 630090.
Translated from Prikladnaya Mekhanika i Tekhnicheskaya Fizika, Vol. 44, No. 4, pp. 83–94, July–August, 2003. Original article submitted January 5, 2003.

leading edges, and by half of a caliber in the case of a plate with a rounded edge. Sparrow et al. [20] also paid much attention to determining the characteristic coordinates of the separated flow around obstacles of different shapes. The authors note that the mismatch of reattachment and maximum heat-transfer points can be rather significant in some cases of separation.

Some experimental works on heat transfer in separated flows have a qualitative character and contain little quantitative information [21]; others deal with only particular problems [22, 23].

An analysis of data published in the literature shows that the mechanism of separated flows is extremely complicated both in the mixing zone with coherent structures and in the recirculation region. Thermal processes are accompanied by violation of the Reynolds analogy between friction and heat transfer. Some features of heat transfer and flow dynamics have not been investigated yet.

In the present work, which is a continuation of [1], we study the thermal characteristics and heat transfer behind a backward-facing step and a rib with identical aerodynamic and geometric characteristics. This allowed us to reveal both the general features of these types of separated flows and their differences.

Test Conditions. The experiments were performed on a setup described in [1] under identical external conditions. The flow velocity above the obstacles was $U_0 = 20$ m/sec, and the obstacle height was $H = 6$, 10, 20, and 30 mm, which corresponded to Reynolds numbers based on the rib or step height $\mathrm{Re}_H = U_0 H/\nu = 8 \cdot 10^3$, $1.33 \cdot 10^4$, $2.66 \cdot 10^4$, and $4 \cdot 10^4$ (ν is the kinematic viscosity). The degree of flow turbulence at the place where the obstacle was located was $\mathrm{Tu}_0 \approx 1.2\%$, and the displacement thickness of the boundary layer was $\delta^* \approx 5.5$ mm. Heated test sections and models were additionally used. The temperature behind the obstacles was measured by 40 Chromel–Copel thermocouples flush-mounted along the plate centerline with a step of 10 mm. The heat flux ($q = \mathrm{const}$) was generated by transmitting alternating electric current over a strip heater located on the plate; the strip heater was made of foil approximately 10 μm thick and had a size of 150×400 mm. The heat flux from the wall q_w was calculated as the difference $q - q_{\mathrm{loss}}$. The heat losses q_{loss} were evaluated by the difference in temperature on the lower and upper surfaces of the plate. The overheating of the surface relative to the main flow $\Delta T = T_w - T_0$ did not exceed 50°C; therefore, the influence of the temperature factor on heat transfer was ignored.

The temperature distribution in the boundary layer was measured by a microthermocouple mounted on a holder introducing the minimum possible perturbations into the flow.

In some experiments, thermovision filming of the heat-exchange surface was performed, which basically confirmed the results obtained in [1] by the oil-film technique, namely, the presence of secondary vortices immediately behind flow separation and also powerful corner vortices at the place where the heat-exchange surface joined the side walls of the channel (see [1, Fig. 2]). Thus, the separated flow formed behind the obstacle is three-dimensional. High temperature gradients in the transverse direction, however, were not observed along the centerline of the heat-exchange surface. This indicates that the flow and the temperature field near the plate centerline, where the main measurements were taken, were quasi-two-dimensional. The results of a series of calibration tests with an attached flow confirmed these conclusions; the heat-transfer coefficients measured in these tests coincided within 5% with the standard dependences for a turbulent boundary layer on a smooth plate.

Measurement Results and Discussion. The distribution of the heat-transfer coefficient along the plate is shown in Fig. 1. The coordinate $x = 0$ corresponds to the place where the obstacle was located. The heat-transfer coefficient was determined by the temperature difference between the wall and the flow core:

$$\alpha = q_w/(T_w - T_0). \tag{1}$$

For comparison, Fig. 1 also shows the results of tests without flow separation (smooth plate without the obstacle).

A decrease in the obstacle height leads to an increase in the heat-transfer maximum (an exception is the data for a step of height $H = 30$ mm, where the relative channel width $W/H < 10$ exerts an effect). The maximum is shifted toward the obstacle. Note, in the case of the step, the length of the recirculation region decreases more intensely and the heat-transfer maximum itself is more clearly expressed. The heat-transfer maximum in the case of flow separation behind the rib (Fig. 1b) is considerably shifted downstream from the separation point.

The information above refers to the results of studying the structure of the separated flow behind the step and the rib.

In the flow around the step (Fig. 1a), the boundary layer in the relaxation region is rapidly recovered to the equilibrium state (except for the test with the step height $H = 30$ mm) and the value of the heat-transfer coefficient coincides with the results measured on the plate. In the flow around the rib (Fig. 1b), such a picture is not observed and the relaxation region is more extended.

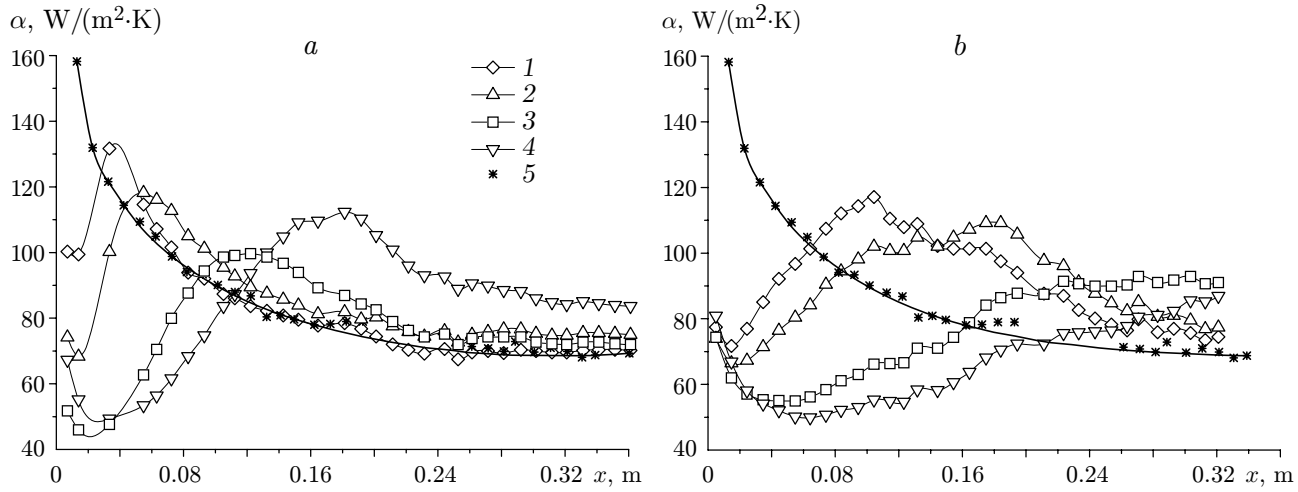

Fig. 1. Distributions of the heat-transfer coefficient behind steps (a) and ribs (b) of different heights: $H = 6$ (1), 10 (2), 20 (3), and 30 mm (4); curve 5 refers to heat transfer on a flat plate.

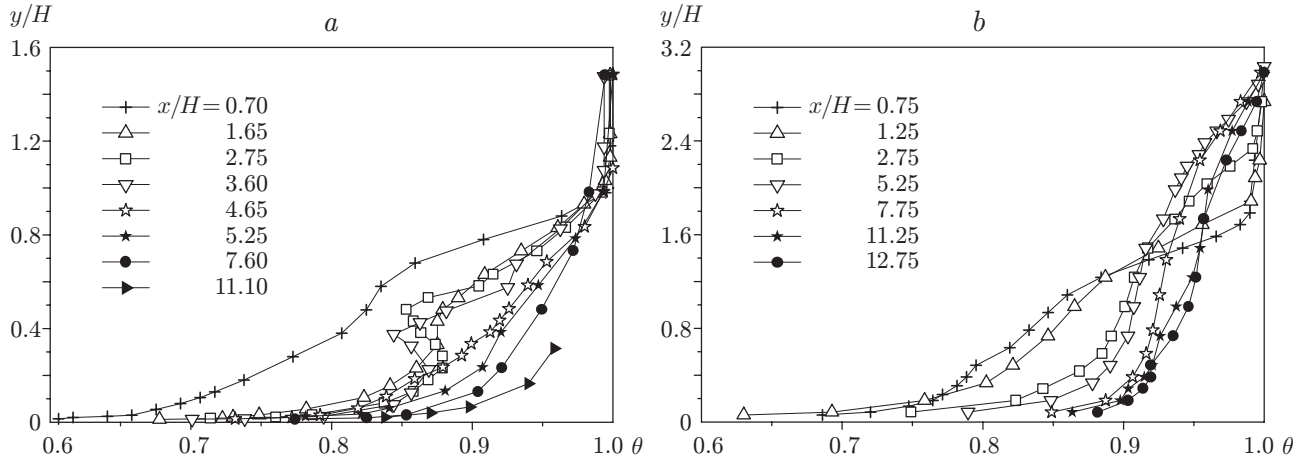

Fig. 2. Profiles of dimensionless temperature behind the step (a) and the rib (b) 20 mm high.

Despite the significant difference in flow structures behind the step and the rib and the difference in pressure in the recirculation region (see [1, Fig. 4]), the maximum values of the heat-transfer coefficient are approximately identical (Fig. 1). This can be explained by the mutual influence of transfer of large-scale structures, which are more pronounced in the case of the flow around the rib, namely, by intensification of heat transfer, on one hand, and by the increase in the boundary-layer thickness responsible for heat-transfer attenuation, on the other hand. The temperature distributions in the form $\theta = (T - T_w)/(T_0 - T_w) = f(y/H)$ plotted in Fig. 2 validate the conclusion made. Indeed, the thickness of the thermal boundary layer and the obstacle height are almost identical in experiments with the step (Fig. 2a), whereas the thermal layer is more than three times thicker in experiments with the rib (Fig. 2b). It follows from Fig. 2 that the main thermal resistance, especially for the step, is concentrated near the wall. An exception is the profiles measured in the recirculation region immediately behind the boundary-layer separation point.

In the flow around the step, a minimum of temperatures is clearly expressed in the mixing layer, which is caused by the vortex transfer of heated volumes of the fluid away from the wall as the flow turns between the primary and secondary vortices. In the flow around the rib, this minimum is weaker expressed because of the thicker mixing layer. Downstream of the reattachment point, the temperature profile gradually acquires the form typical of the temperature distribution in a turbulent boundary layer.

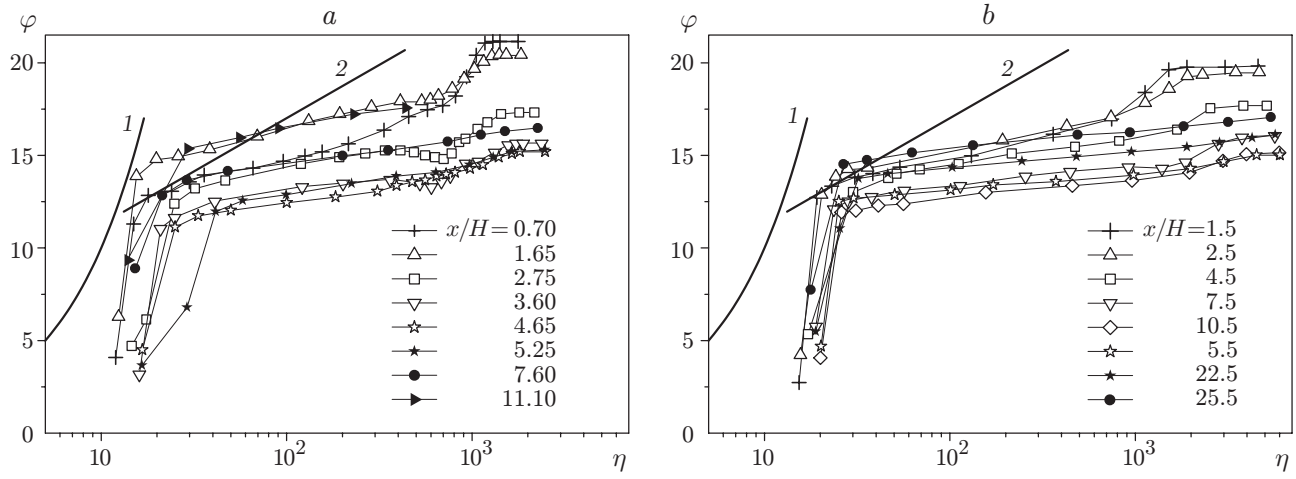

Fig. 3. Temperature profiles in universal coordinates behind the step 20 mm high (a) and behind the rib 10 mm high (b): curves 1 and 2 refer to the temperature distributions in the laminar sublayer and in the turbulent core, respectively.

The temperature profiles processed in universal coordinates are plotted in Fig. 3. Since skin friction was not measured in the experiments, the characteristic parameter in processing the results was the thermal analog of the friction velocity $\theta^* = (T_0 - T_w)\sqrt{\mathrm{St}}$ (St is the Stanton number). In Fig. 3, we have

$$\varphi = \frac{T - T_w}{T_0 - T_w}\,\frac{1}{\sqrt{\mathrm{St}}}, \qquad \eta = yU_0\,\frac{\sqrt{\mathrm{St}}}{\nu}.$$

Curves 1 and 2 refer to the temperature distributions in the laminar sublayer and turbulent core of the boundary layer:

$$\varphi = \eta, \qquad \varphi = 2.5\ln\eta + 5.5. \tag{2}$$

It follows from Fig. 3 that the temperature profiles measured both for the step and for the rib differ from the standard distribution, which indicates different mechanisms of heat transfer in the turbulent core and in the buffer and laminar zones. The experimental points are located much lower than the curves of Eq. (2), and significant scatter of data for different values of x/H is observed. The slope of the curves approximating experimental data is substantially smaller in the logarithmic region than in the standard boundary layer, which indicates the attenuation of heat-transfer processes in the turbulent core in the case of flow separation. Nevertheless, the logarithmic sector of the temperature profile of the separated flow does exist, which can be important for the development of the corresponding models of turbulent transfer.

In the case of flow stalling from the step edge (Fig. 3a), a tendency to reconstruction of the equilibrium temperature profile is observed at large distances from the separation point, and the experimental points in the turbulent core approach the dependence for the standard boundary layer. The difference persists in the wake region, which indicates the strong influence of the mixing layer formed during separation on the temperature distribution.

Generalization of Experimental Data on Heat Transfer of the Separated Flow. The most important characteristics of heat transfer in a separated flow are the maximum value of heat transfer and the coordinate of the maximum. Therefore, these parameters are used as scales in most existing methods based on empirical generalization of heat-transfer data [10–12, 19–21, 24].

In a dimensionless form, Fig. 4 shows most of the available data on heat transfer behind steps and ribs and also the data of the present work ($x_{\alpha_{\max}}$ is the coordinate of the heat-transfer maximum and δ is the boundary-layer thickness). In the vicinity of the separation point $[-0.5 \leqslant (x - x_{\max})/x_{\max} \leqslant 0.5]$, the experimental results obtained in a wide range of Reynolds numbers and step heights are rather close. The greatest difference is observed in the recirculation region, where the influence of secondary (essentially three-dimensional) vortex flows near the obstacle base is observed. The difference in experimental data is also observed in the relaxation region, though here it does not exceed 20–30%.

The dependence of the maximum Nusselt number ($\mathrm{Nu}_{\max} = \alpha_{\max}L/\lambda$, where λ is the thermal conductivity) behind the step and the rib on the Reynolds number ($\mathrm{Re}_L = U_0L/\nu$) is plotted in Fig. 5. The linear

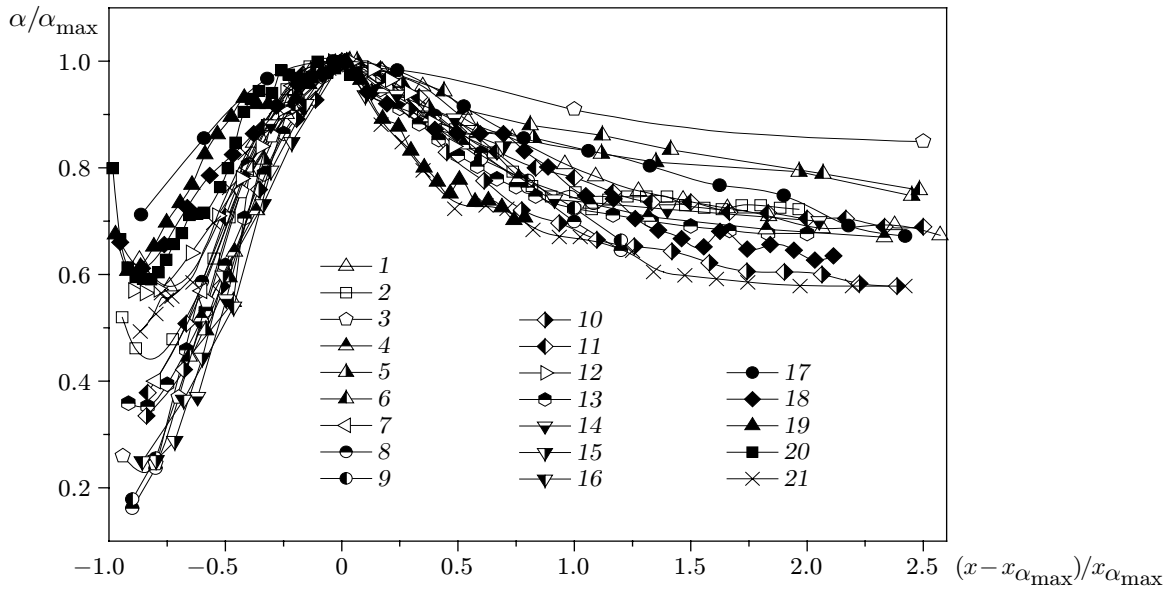

Fig. 4. Distributions of the heat-transfer coefficient behind steps (1–16) and ribs (17–21) of various heights: $H = 10$ mm (1), $H = 20$ mm (2), $H = 3.3$ mm (3) [23], $H = 4.8$ mm (4–6) [10] [Re = 35,400 (4), Re = 56,800 (5), and Re = 87,700 (6)], $H = 25.4$ mm (7) [6], data of [25] (8–9) [Re = 626.78 (8) and Re = 1728.4 (9)], $H = 38$ mm (10, 11) [8] [$\delta/H = 0.15$ (10) and 1.1 (11)], $H = 42$ mm (12) [13], $H = 50$ mm (13) [17], $H = 25$ mm (14) [26], $H = 50$ mm (15) [26], $H = 100$ mm (16) [26], $H = 3$ mm (17), $H = 6$ mm (18), $H = 10$ mm (19), $H = 20$ mm (20), and $H = 15$ mm (21) [19].

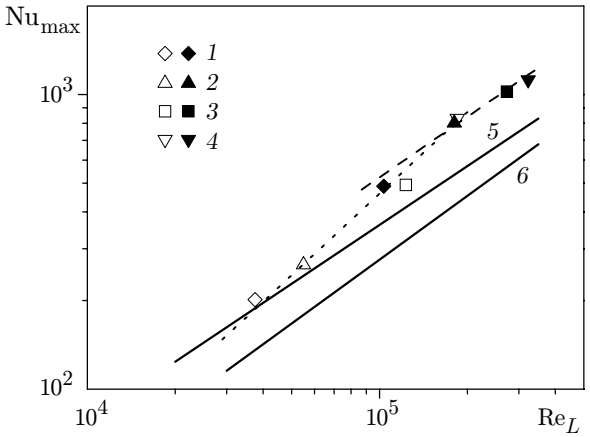

Fig. 5. Maximum Nusselt number behind the step (open points) and behind the rib (filled points) for $H = 6$ (1), 10 (2), 20 (3), and 30 mm (4); curves refer to the calculations by empirical formulas $\mathrm{Nu}_L = 0.192\,\mathrm{Re}_L^{0.665}\,\mathrm{Pr}^{1/3}$ (5) and $\mathrm{Nu}_L = 0.0803\,\mathrm{Re}_L^{0.72}\,\mathrm{Pr}^{0.43}$ (6).

scale was the distance from the separation point to the reattachment point, which was calculated by the formula $L = \sqrt{H^2 + x_{\alpha_{\max}}^2}$. The velocity U_0 was specified directly above the step and the rib. For comparison, Fig. 5 also shows the results calculated by empirical formulas from [11]

$$\mathrm{Nu}_L = 0.0803\,\mathrm{Re}_L^{0.72}\,\mathrm{Pr}^{0.43}$$

and [12]

$$\mathrm{Nu}_L = 0/192\,\mathrm{Re}_L^{0.665}\,\mathrm{Pr}^{1/3} \tag{3}$$

(Pr is the Prandtl number).

It should be noted that the Reynolds number in Eq. (3) is calculated on the basis of the velocity along the outer boundary of the separated shear layer. For gradient flows, this velocity differs from the free-stream velocity

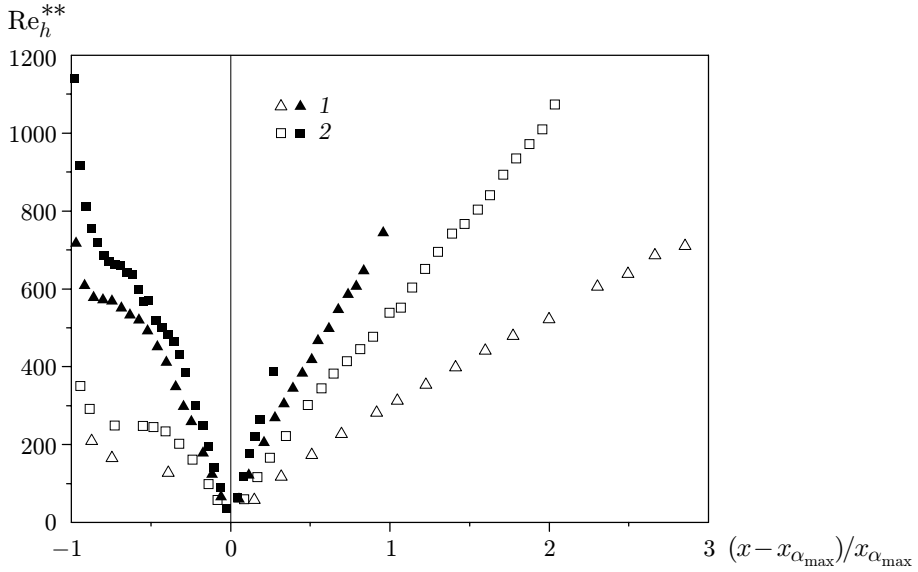

Fig. 6. Distribution of the thermal Reynolds number behind the step (open points) and behind the rib (filled points) upstream and downstream of the point of maximum heat transfer for $H = 10$ (1) and 20 mm (2).

upstream of the obstacle and characterizes, to a certain extent, the difference in parameters of the separated flows behind the step and the rib.

It follows from Fig. 5 that the experimental data for the step at low Reynolds numbers are in good agreement with the calculation results obtained by the empirical formula (3); for ribs, the difference is more substantial, and the distribution of $\mathrm{Nu}_{\max}$ corresponds to the turbulent flow character more exactly.

A promising approach to the analysis of heat transfer in separated flows was proposed in [5, 11, 27]. The approach is based on an independent consideration of recirculation and relaxation flows. It is assumed that the boundary-layer thickness is zero at the reattachment point, and the boundary layers developing upstream and downstream of this point can be described by the boundary-layer theory relations.

Figure 6 shows the distribution of the Reynolds number based on the energy-loss thickness along the x axis. In the experiments, the thermal Reynolds number was determined by the relation derived by solving the integral equation of energy for the case $q_w = \mathrm{const}$:

$$\mathrm{Re}_h^{**} = \frac{q_w}{\Delta T c_p \mu}\, x \tag{4}$$

(c_p is the heat capacity and μ is the dynamic viscosity).

At the first stage of the analysis, the values of Re_h^{**} were calculated on the basis of the free-stream parameters; therefore, the temperature difference was determined as $\Delta T = T_w - T_0$. The x coordinate in Eq. (4) was counted from the point of heat-transfer maximum in the upstream direction (negative values of x correspond to the recirculation region) and in the downstream direction (positive values of x correspond to the relaxation region).

The data in Fig. 6 should be analyzed together with the heat-transfer coefficient distributions (see Fig. 1). In the case of flow separation behind the step, owing to the small length of the vortex region, the thermal Reynolds number near the obstacle base does not exceed the value $\mathrm{Re}_h^{**} \approx 300$ typical of the laminar–turbulent transition on a flat plate. For ribs, the Reynolds number reaches $\mathrm{Re}_h^{**} > 1000$, which corresponds to a developed turbulent thermal layer (see Fig. 6).

The linear scale of the separation region exerts a determining effect on the distribution of the thermal Reynolds number in the relaxation region as well. The thermal layer on the measurement sector behind a step of large height has enough time to develop ($\mathrm{Re}_h^{**} \approx 1000$), which is not observed for ribs.

The results of processing of experimental data on the heat-transfer coefficient are plotted in Fig. 7. As in Fig. 6, the x coordinate was counted from the position of the heat-transfer maximum. The heat-transfer coefficient was calculated from the temperature difference between the wall and the flow core [see formula (1)] and the Reynolds number Re_x was based on the free-stream velocity above the obstacle. For comparison, Fig. 7 also shows the calculated dependences corresponding to heat transfer in standard laminar and turbulent boundary layers.

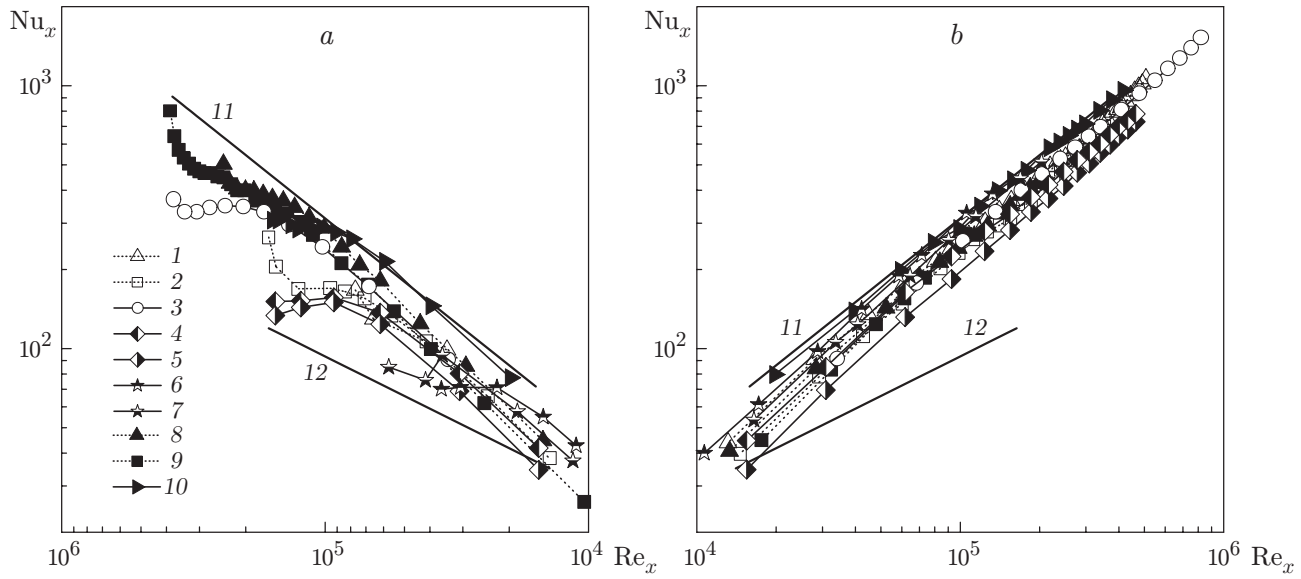

Fig. 7. Heat transfer behind the step (1–7) and behind the rib (8–10) in the recirculation (a) and relaxation (b) regions: $H = 10$ (1, 8), $H = 20$ mm (2, 9), $H = 50$ mm (3) [17], $H = 38$ (4, 5) [8] ($\delta/H = 0.15$ (4) and $\delta/H = 1.1$ (5)), $H = 5$ mm (6, 7) [10] [$U_0 = 25.8$ (6) and 39.8 m/sec (7)], $H = 15$ mm (10) [19]; curves are the calculated dependences for $\mathrm{Nu}_x = 0.036\,\mathrm{Re}_x^{0.8}\,\mathrm{Pr}^{\,0.4}$ (11) and $0.332\,\mathrm{Re}_x^{0.5}\,\mathrm{Pr}^{\,1/3}$ (12)].

Despite the significant scatter of experimental data, possible reasons for which were discussed above, the experimental points in the relaxation region are generalized by the dependence typical of the turbulent flow regime. Most experimental data with a scatter within 20% correspond to the heat-transfer law in the standard turbulent attached flow $\mathrm{Nu}_x = 0.036\,\mathrm{Re}_x^{0.8}\,\mathrm{Pr}^{\,0.4}$.

In the recirculation region (Fig. 7a), the situation is more complicated. The experimental points are located between the curves corresponding to the laminar and turbulent heat transfer. In such an interpretation, therefore, it is difficult to evaluate the flow character.

The situation it also aggravated by the fact that the technique for data processing with the use of free-stream parameters, which was used to plot Fig. 7, ignores the features of the reverse vortex flow in the recirculation region. In this region, the reattachment point is the starting point for the boundary layer whose flow is similar to the flow in the near-wall ambient jet. Therefore, the experimental data in this region were processed with the use of parameters at the boundary of the near-wall region, where the reverse flow velocity reaches the maximum value. The experimental data for the thermal problem in [11] and for the dynamic problem in [28] were treated in a similar manner.

The results of data processing for the recirculation region by the method described are plotted in Fig. 8. The Reynolds number was determined by the maximum velocity of the near-wall reverse flow ($\mathrm{Re}_{x,m} = U_{\max} x/\nu$), and the heat-transfer coefficient was calculated by the temperature difference between the wall and the cross section corresponding to the maximum velocity: $\alpha_m = q_w/(T_w - T_{\max})$. In Fig. 8, we have $\mathrm{Nu}_{x,m} = \alpha_m x/\lambda$.

It follows from Fig. 8 that the experimental data in this interpretation do not coincide with the dependences for the laminar and turbulent flow regimes in the boundary layer, though the slope of the curve $\mathrm{Nu}_{x,m}(\mathrm{Re}_{x,m})$ corresponds more to the turbulent law of heat transfer. This conclusion contradicts the results of [28], where the data on skin friction were found to be in good agreement with the dependence for the laminar flow regime. One of the main reasons for flow laminarization, in the opinion of Adams and Johnson [28], is the strong influence of the stabilizing streamwise acceleration of the flow. The estimates show that the values of the acceleration parameter under the present test conditions exceeds the critical value by an order of magnitude, but no laminarization of heat transfer is observed. This interesting and important fact is, possibly, related to the high level of turbulence in the mixing layer and requires a more detailed study.

Intensification and Reduction of Heat Transfer Behind the Step and the Rib. For practical applications, it is important to know the degree of heat-transfer intensification or, vice versa, reduction in the case of flow separation behind obstacles of various heights. For this purpose, the experimental data obtained were presented as the ratio of the mean heat-transfer coefficients with separation behind an obstacle and in the absence

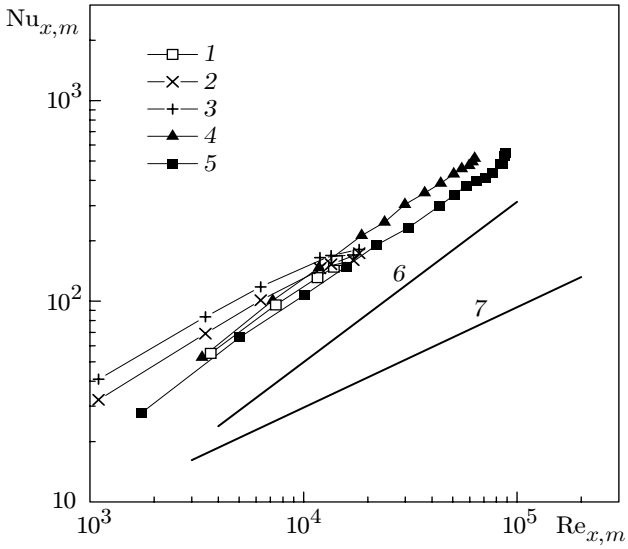

Fig. 8. Generalization of data on heat transfer behind the step (1–3) and behind the rib (4 and 5) in the recirculation region with the use of near-wall flow parameters: $H = 20$ (1, 5), 38 (2, 3) [8] [$\delta/H = 0.15$ (2) and 1.1 (3)], and 10 mm (4); curves are the calculated dependences for $\mathrm{Nu}_x = 0.036\,\mathrm{Re}_x^{0.8}\,\mathrm{Pr}^{0.4}$ (6) and $0.332\,\mathrm{Re}_x^{0.5}\,\mathrm{Pr}^{1/3}$ (7).

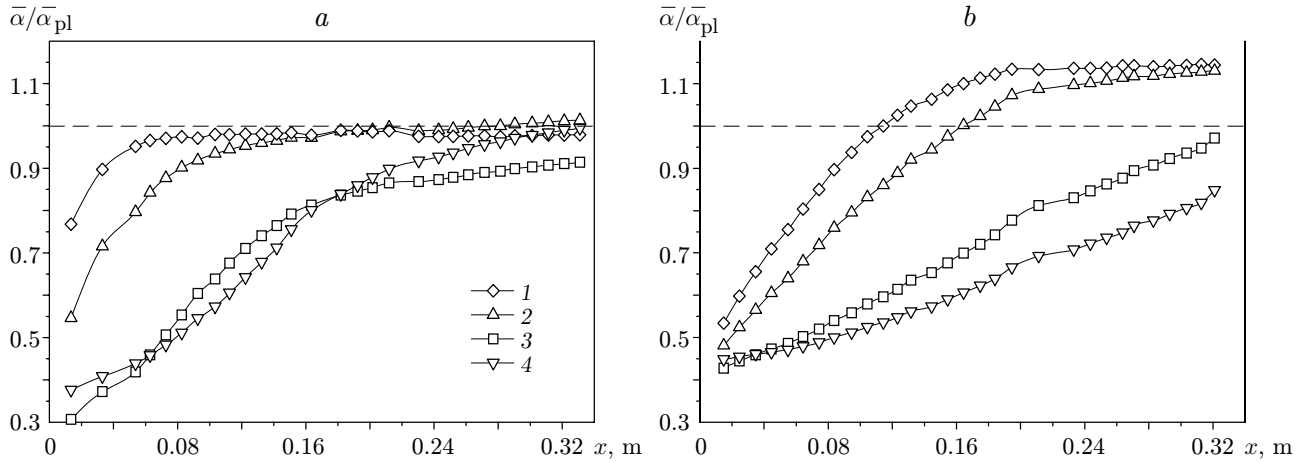

Fig. 9. Effect of the step (a) and the rib (b) on the mean heat-transfer coefficient: $H = 6$ (1), 10 (2), 20 (3), and 30 mm (4).

of the obstacle (smooth plate). The results of data processing are presented in Fig. 9. Only at distances equal to 10–20 heights of the obstacle is the heat transfer recovered to the level corresponding to an attached flow past the plate. The intensifying action of the rib is manifested for $x/H \geqslant$ 10–20 (the maximum value is $\bar{\alpha}/\bar{\alpha}_{\mathrm{plate}} \approx 1.15$). These results were obtained for ribs of small heights ($H = 6$ and 10 mm). In experiments with higher ribs, the channel length was insufficient for determining the maximum value of the heat-transfer coefficient. It is obvious, nevertheless, that such ribs cannot play the role of heat-transfer intensifiers because of the large length of the reduced heat-transfer region.

Conclusions. A comparative analysis of experimental data on heat transfer in a separated flow behind steps and ribs of various heights is performed. It is shown that the heat-transfer maximum behind the step increases more significantly with decreasing obstacle height than that behind the rib. The temperature profile behind the step in the recirculation region has a clearly expressed inflection. The experimental data on heat transfer in the separation region, being processed with the use of parameters at the inner boundary of the primary vortex, obey the laws for the turbulent flow. An exception is the data for the secondary vortex region. Only ribs of height lower than 10 mm serve as heat-transfer intensifiers.

This work was supported by the Russian Foundation for Fundamental Research (Grant 01-02-16842a).

REFERENCES

1. V. I. Terekhov, N. I. Yarygina, and R. F. Zhdanov, "Some features of a turbulent separated flow and heat transfer behind a step and a rib. 1. Flow structure," *J. Appl. Mech. Tech. Phys.*, **43**, No. 6, 877–887 (2002).
2. R. L. Simpson, "A review of some phenomena in turbulent flow separation," *Trans. ASME, J. Fluid Eng.*, **102**, No. 4, 520–533 (1981).
3. J. K. Eaton and J. P. Johnston, "A review of research on subsonic turbulent flow reattachment," *AIAA J.*, **19**, 1093–1105 (1981).
4. R. B. Shlyazhas, "Turbulent momentum and heat transfer in the boundary layer behind an obstacle," Candidate's Dissertation in Technical Sciences, Inst. of Physicotechnical Problems in Power Engineering, Kaunas (1984).
5. V. I. Terekhov, "Separated flows: formation mechanisms and possibility of heat-transfer control," in: *Physical Fundamentals of Experimental and Mathematical Modeling of Gas Dynamics and Heat and Mass Transfer in Energy Facilities* [in Russian], Vol. 1, Moscow Inst. of Power Eng., Moscow (2001), pp. 15–20.
6. R. A. Seban, "Heat transfer to the turbulent separated flow of air downstream of a step in the surface of a plate," *Trans. ASME, J. Heat Transfer*, **86**, No. 2, 259–264 (1964).
7. E. G. Filetti and W. M. Kays, "Heat transfer in separated, reattached, and redevelopment regions behind a double step at entrance to a flat duct," *Trans. ASME, J. Heat Transfer*, **89**, No. 2, 163–167 (1967).
8. J. C. Vogel and J. K. Eaton, "Combined heat transfer and dynamic measurements downstream of a backward-facing step," *Trans. ASME, J. Heat Transfer*, **107**, No. 4, 922–929 (1985).
9. M. G. Ktalkherman, "Heat transfer to a plate behind an obstacle," *J. Appl. Mech. Tech. Phys.*, No. 5, 93–95 (1966).
10. P. L. Komarov and A. F. Polyakov, "Turbulence and heat-transfer characteristics behind a backward-facing step in a slotted channel," Preprint No. 2-396, Inst. of High Temp., Russian Acad. of Sci., Moscow (1996).
11. A. I. Leont'ev, V. I. Ivin, and L. V. Grekhov, "Semi-empirical method for evaluating the heat-transfer level behind the boundary-layer separation point," *Inzh.-Fiz. Zh.*, **47**, No. 4, 543–550 (1984).
12. T. Ota and H. Nishiyama, "A correlation of maximum turbulent heat transfer coefficient in reattachment flow region," *Int. J. Heat Mass Transfer*, **30**, No. 6, 1193–1200 (1987).
13. V. E. Alemasov, G. A. Glebov, and A. P. Kozlov, *Hot-Wire Methods of Investigating Separated Flows* [in Russian], Kazan' Department of the Academy of Sciences of the USSR, Kazan' (1989).
14. N. Kasagi, M. Hirata, and H. Hiraoka, "Transport mechanism in separated flow around a downward step," in: Proc. of the 14th Nat. Heat Transfer Symp. of Japan, Univ. of Tokyo Press, Tokyo (1977), pp. 76–78.
15. T. Kawamura, S. Tanaka, I. Mabuchi, and M. Kumada, "Temporal and spatial characteristics of heat transfer at the reattachment region of a backward-facing step," *Exp. Heat Transfer*, **1**, 299–313 (1987/1988).
16. J. W. Bon, M. A. Hoffmann, B. E. Launder, et al., "Heat transfer, temperature, and velocity measurements downstream of an abrupt expansion in a circular tube at a uniform wall temperature," *Trans. ASME, J. Heat Transfer*, **111**, No. 4, 870–877 (1989).
17. T. Ota and Y. Sugawara, "Turbulent heat transfer on the separated and reattached flow around an inclined downward step," in: *Proc. of the 10th Int. Heat Transfer Conf.* (Brighton, UK, August 14–18, 1994), Vol. 3, IChemE, London (1994), pp. 113–118.
18. T. Ota and N. Kon, "Heat transfer in the separated and reattached flow on a blunt flat plate," *Trans. ASME, J. Heat Transfer*, **96**, No. 4, 459–462 (1974).
19. E. R. Dyban, É. Ya. Épik, and L. E. Yushina, "Heat transfer on a streamwise flow on a flat plate with separation and turbulization of external flow," *Prom. Teplotekh.*, **17**, Nos. 1–3, 3–12 (1995).
20. E. M. Sparrow, S. S. Kang, and W. Chuck, "Relation between the points of flow reattachment and maximum heat transfer for region of flow separation," *Int. J. Heat Mass Transfer*, **30**, No. 7, 1237–1246 (1987).
21. N. Seki, S. Fukusako, and T. Hirata, "Turbulent fluctuations and heat transfer for separated flow associated with a double step at entrance to an enlarged flat duct," *Trans. ASME, J. Heat Transfer*, **98**, No. 4, 588–593 (1976).
22. P. P. Zemanik and R. S. Dugall, "Local heat transfer downward of abrupt circular channel expansion," *Trans. ASME, J. Heat Transfer*, **92**, No. 1, 54–62 (1970).
23. F. K. Tsou, Sh. Chen, and W. Aung, "Starting flow and heat transfer downstream of a backward-facing step," *Trans. ASME, J. Heat Transfer*, **113**, No. 3, 583–590 (1991).
24. A. Pyadishyus and A. Shlanchyauskas, *Turbulent Heat Transfer in Near-Wall Layers* [in Russian], Mokslas, Vil'nyus (1987).

25. W. Aung and R. J. Goldstein, "Heat transfer in turbulent separated flow downstream of a rearward-facing step," *Israel J. Tech.*, **10**, 35–41 (1972).
26. V. P. Solntsev, V. N. Kryukov, and I. A. Matveev, "Investigation of heat transfer in the separation region behind a planar step," in: *Fundamentals of Heat Transfer in Aviation and Rocket-Space Engineering* [in Russian], Mashinostroenie, Moscow (1975), pp. 513–518.
27. V. I. Terekhov, N. I. Yarygina, and R. F. Zhdanov, "Effect of high turbulence and obstacle geometry on the structure and thermal characteristics of the separated flow," in: *Proc. Russian National Symposium on Power Engineering* (Kazan', September 10–14, 2001), Vol. 1, Kazan' State University of Power Engineering, Kazan' (2001), pp. 417–421.
28. A. W. Adams and J. P. Johnston, "Flow structure in the near-wall zone of turbulent separated flow," *AIAA J.*, **26** No. 5, 932–939 (1988).